Journal of Cerebral Blood Flow & Metabolism (2012) 32, 447–455

www.jcbfm.com

Experimental subarachnoid hemorrhage causes early and long-lasting microarterial constriction and microthrombosis: an *in-vivo* microscopy study

Benjamin Friedrich[1], Frank Müller[1], Sergej Feiler[1], Karsten Schöller[1,2] and Nikolaus Plesnila[1,3,4]

[1]*Institute for Surgical Research, University of Munich Medical Center-Großhadern, Ludwig-Maximilians University, Munich, Germany;* [2]*Department of Neurosurgery, University of Munich Medical Center-Großhadern, Ludwig-Maximilians University, Munich, Germany;* [3]*Royal College of Surgeons in Ireland, Dublin, Ireland*

Early brain injury (EBI) after subarachnoid hemorrhage (SAH) is characterized by a severe, cerebral perfusion pressure (CPP)-independent reduction in cerebral blood flow suggesting alterations on the level of cerebral microvessels. Therefore, we aimed to use *in-vivo* imaging to investigate the cerebral microcirculation after experimental SAH. Subarachnoid hemorrhage was induced in C57/BL6 mice by endovascular perforation. Pial arterioles and venules (10 to 80 μm diameter) were examined using *in-vivo* fluorescence microscopy, 3, 6, and 72 hours after SAH. Venular diameter or flow was not affected by SAH, while >70% of arterioles constricted by 22% to 33% up to 3 days after hemorrhage ($P<0.05$ versus sham). The smaller the investigated arterioles, the more pronounced the constriction ($r^2=0.92$, $P<0.04$). Approximately 30% of constricted arterioles were occluded by microthrombi and the frequency of arteriolar microthrombosis correlated with the degree of constriction ($r^2=0.93$, $P<0.03$). The current study demonstrates that SAH induces microarterial constrictions and microthrombosis *in vivo*. These findings may explain the early CPP-independent decrease in cerebral blood flow after SAH and may therefore serve as novel targets for the treatment of early perfusion deficits after SAH.
Journal of Cerebral Blood Flow & Metabolism (2012) **32,** 447–455; doi:10.1038/jcbfm.2011.154; published online 7 December 2011

Keywords: intravital microscopy; microcirculation; microthrombosis; mice; subarachnoid hemorrhage; vasospasm

Introduction

Subarachnoid hemorrhage (SAH) is a subtype of stroke with a particularly high morbidity and mortality. In all, 25% of patients die almost immediately after hemorrhage due to arrest of the cerebral circulation caused by acute intracranial hypertension as a consequence of the evolving hematoma (Pobereskin, 2001). Out of the remaining 75% of SAH victims, 15% die with a significant delay of several days (due to delayed cerebral ischemia or cardiopulmonary reasons); however, the remaining 60% of patients die within 48 h of the initial bleeding (Weir *et al*, 1978; Harrod *et al*, 2005) due to rebleedings (25%) or a sequence of events summarized by the term ''Early Brain Injury'' (EBI; 35%) (Pobereskin, 2001). While rebleedings can be prevented by surgical or endovascular procedures and, after years of research, new therapeutic options are emerging for the intriguing phenomenon of delayed cerebral ischemia, no treatment is available for EBI and its underlying mechanisms have only recently started to be understood (Cahill and Zhang, 2009; Pluta *et al*, 2009).

In patients, EBI usually occurs within the first 2 days after the initial bleed, i.e., well before the presence of macrovasospasm, which usually starts 5 to 8 days after SAH. One of the main characteristics of EBI is a severe reduction in cerebral blood flow (Schubert *et al*, 2009) and subsequent ischemic brain damage (Adams *et al*, 1981) under conditions of normal or almost normal cerebral perfusion pressure (CPP). Hence, ischemia has to be caused by the constriction of vessels on the level of the cerebral microcirculation, as previously

Correspondence: Professor Dr N Plesnila, Experimental Stroke Research, Institute for Stroke and Dementia Research (ISD), University of Munich Medical School—Campus Großhadern Max-Lebsche Platz 30, 81377 Munich, Germany.
E-mail: nikolaus.plesnila@med.uni-muenchen.de
[4]Current address: Institute for Stroke and Dementia Research, University of Munich Medical Center-Großhadern, Ludwig-Maximilians University, Munich, Germany.
The current work was supported by the German Research Foundation (DFG; SCHO 1385/1-1).
Received 3 May 2011; revised 18 July 2011; accepted 14 August 2011; published online 7 December 2011

demonstrated in experimental animals (Herz *et al*, 1975; Sehba *et al*, 2007; Sun *et al*, 2009) and in patients (Uhl *et al*, 2003; Pennings *et al*, 2004).

The sequence of events resulting in these early microvascular constrictions has been investigated by a series of elegant experimental studies using histological and imaging techniques and seems to start with an acute vasoconstriction of vessels at the scull base (the internal carotid artery, the anterior cerebral artery, and their A2 branches) as early as 5 minutes after SAH (Bederson *et al*, 1998; Sehba *et al*, 1999); this is followed by an acute constriction of intraparenchymal and pial microvessels (10 to 30 μm) up to 24 hours after SAH (Sehba *et al*, 2007; Sun *et al*, 2009). So far, however, most of these investigations were performed on fixed tissue (Bederson *et al*, 1998; Sehba *et al*, 1999, 2005, 2007) or only acutely (< 2 hours) after SAH (Sun *et al*, 2009). Accordingly, little is known about the long-term spatial and temporal characteristics of post hemorrhagic microvascular constriction in the *in-vivo* situation. Therefore, the aim of the current study was to investigate subarachnoid microvessels, up to 3 days after SAH, by *in-vivo* microscopy and to evaluate potential dynamic interactions between cerebral microconstrictions, thrombus formation, and cerebral blood flow, to better understand the mechanisms responsible for early ischemia after SAH.

Materials and methods

Male C57Bl6 mice (23 to 25 g body weight, $n = 28$) were used for the current study. Experimental animals were purchased from Charles River Laboratory (Sulzfeld, Germany) and cared for before and at all stages of the experiment in compliance with the institutional guidelines and regulations of the Animal Care Committee of the District Government of Upper Bavaria (Protocol Number Az 55.2-1-54-2531-118-05).

Animal Preparation and Monitoring

Animals had free access to food and water before surgery. Anesthesia was induced by intraperitoneal injection of midazolam (5 mg/kg; Ratiopharm, Ulm, Germany), fentanyl (0.05 mg/kg; CuraMed, Karlsruhe, Germany), and medetomidine (0.5 mg/kg; Pfizer, Karlsruhe, Germany) and was maintained by hourly injections of one quarter of the initial dose as previously described (Thal and Plesnila, 2007). Mice were oro-trachealy intubated and mechanically ventilated with 35% O_2 in room air (Minivent, Hugo Sachs, Hugstetten, Germany). End-tidal pCO_2 was measured with a microcapnometer (C1240, Columbus Instruments, Columbus, OH, USA) and kept constant between 35 and 45 mm Hg by respective adjustments of ventilation. A thermostatically regulated, feedback-controlled heating pad (FHC, Bowdoinham, ME, USA) was used to maintain body temperature at 37°C. Intracranial pressure (ICP) was measured in each animal for 15 minutes after SAH using a microchip-based pressure transducer (Johnson & Johnson Medical Limited, Berkshire, UK) to prove successful induction of SAH as recently described in detail (Feiler *et al*, 2010). Blood gases and electrolytes were determined at the end of each experiment (Table 1).

Table 1 Mean arterial blood pressure (MAP), blood gases, and electrolytes during intravital microscopy

	Sham		*SAH*	
	15 minutes	*90 minutes*	*15 minutes*	*90 minutes*
MAP (mm Hg)	72 ± 12	64 ± 11	68 ± 7	66 ± 10
pH (a.u.)	—	7.2 ± 0.06	—	7.2 ± 0.02
pCO_2 (mm Hg)	—	54 ± 2	—	48 ± 2
pO_2 (mm Hg)	—	102 ± 15	—	112 ± 9
HCO_3^- (mmol/L)	—	21 ± 3	—	20 ± 1
Hb sat (%)	—	95 ± 1	—	96 ± 1
Na^+ (mmol/L)	—	147 ± 2	—	149 ± 1
K^+ (mmol/L)	—	5.0 ± 0.5	—	4.9 ± 0.4
Ca^{2+} (mmol/L)	—	1.4 ± 0.1	—	1.4 ± 0.1
Cl^- (mmol/L)	—	113 ± 1	—	117 ± 1
Glucose (mg/dL)	—	238 ± 4	—	223 ± 18

Induction of Subarachnoid Hemorrhage

Subarachnoid hemorrhage was induced using the endovascular perforation technique as described previously (Feiler *et al*, 2010; Schöller *et al*, 2011). Briefly, a 5-0 monofilament was introduced via the left external carotid artery into the internal carotid artery and advanced intracranially. Successful SAH induction was proven by a sudden sharp increase in ICP. Immediately, thereafter the filament was withdrawn and the external carotid artery was ligated. In sham-operated animals, the filament was introduced into the internal carotid artery and advanced intracranially, but no SAH was induced. Anesthesia was terminated by intraperitoneal injection of atipamezole (2.5 mg/kg; Pfizer), naloxone (1.2 mg/kg; Inresa, Freiburg, Germany), and flumazenil (0.5 mg/kg; Hoffmann-La-Roche, Grenzach-Wyhlen, Germany). Thereafter, animals were kept in an incubator at 33°C for up to 24 hours.

Intravital Fluorescence Microscopy

Intravital microscopy was performed as previously described (Kataoka *et al*, 2004; Schwarzmaier *et al*, 2010). Briefly, animals were reanesthetized and a cranial window (2 × 2 mm) was drilled above the left hemisphere (Figure 1A). The microcirculation was visualized by intravenous injection of 0.15 ml fluoresceinisothiocyanate [FITC]-dextran (MW 150 kDa; Sigma, Deisenhofen, Germany). The entire vascular tree of the ipsilateral middle cerebral artery (MCA) (vessel diameter: 10 to 80 μm; 12 to 32 vessel segments per mouse) was investigated in each animal. Each segment was evaluated every 15 minutes for 10 seconds. A total of 466 vessel segments (each possibly containing more than one constricted section) were investigated. Images were recorded on videotapes and analyzed offline by a blinded investigator.

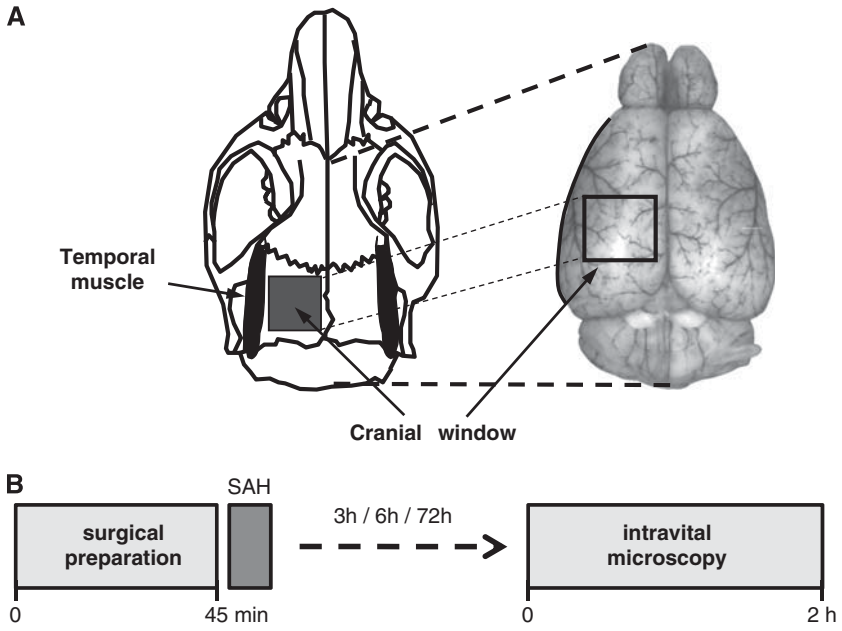

Figure 1 (**A**) Schematic drawing of the location of the cranial window used for intravital microscopy. (**B**) Schematic drawing of the experimental protocol used in the present study. Anesthesia was discontinued after subarachnoid hemorrhage (SAH) and mice were reanesthetized at different time points after SAH for intravital fluorescence microscopy.

Analysis of the Pial Microvasculature

Vessel diameters were quantified with a custom-made image analysis software (CapImage, Heidelberg, Germany) as previously described (Kataoka *et al*, 2004; Schwarzmaier *et al*, 2010). Individual vessel constrictions were analyzed by dividing the diameter of the most constricted vessel segment (Figure 2B, white solid arrow) by the diameter of the nearest not constricted vessel segment (Figure 2B, dotted arrow bottom). For graphical and statistical representation, vessels were grouped by their nonconstricted diameters into four categories ($<20\,\mu$m, 20 to 30 μm, 30 to 40 μm, and 40 to 80 μm). To validate that not constricted appearing vessel segments indeed represented the baseline diameter of this vessel, microvessels were categorized by their degree of branching from the MCA (A1 to A6) (Strahler, 1944) and the mean diameter of each category was calculated and compared between sham-operated mice and mice subjected to SAH. No difference was detected between groups indicating that nonconstricted vessel segments in mice subjected to SAH indeed represented the physiological baseline (data not shown). Microthrombosis was identified by lack of microvascular perfusion together with the massive accumulation of FITC-dextran-stained platelets (Figure 2B, dotted arrow top).

Experimental Protocol

Four experimental groups were investigated by intravital microscopy: (1) 3 hours after sham surgery ($n=6$), (2) 3 hours after SAH ($n=6$), (3) 6 hours after SAH ($n=8$), and (4) 72 hours after SAH ($n=8$; Figure 1B). Animals that died due to SAH were replaced. At the end of the experiment, animals were killed by cervical dislocation in deep anesthesia.

Statistical Analysis

Statistical analysis was performed with SigmaStat 3.1 (SPSS Science, Chicago, IL, USA). Data were analyzed with Kruskal–Wallis analysis of variance on ranks followed by Dunn's method as *post hoc* test. Data on microthrombi were analyzed using a χ^2-test. For correlations, the Pearson Product Moment test was used. Statistical significance was assumed at $P<0.05$. Data are presented as mean values ± s.d., if not otherwise indicated.

Results

Monitoring and Mortality

Subarachnoid hemorrhage resulted in an immediate and steep increase in ICP to 60 ± 6 mm Hg (mean ± s.e.m.), indicating a comparable severity of SAH in all animals investigated. The overall mortality was 29% (9/31), well in agreement with our previously published results in C57/BL6 mice (Feiler *et al*, 2010; Schöller *et al*, 2011).

After intravital microscopy, physiological parameters (mean arterial blood pressure, blood gases, electrolytes, and blood glucose) did not differ between SAH and sham-operated animals, indicating comparable physiological conditions in all investigated animals (Table 1).

Distribution of Blood

After SAH, blood spread within the subarachnoid space at the base of the skull and reached the apical cerebral cortex (Figure 2A). Interestingly, the blood

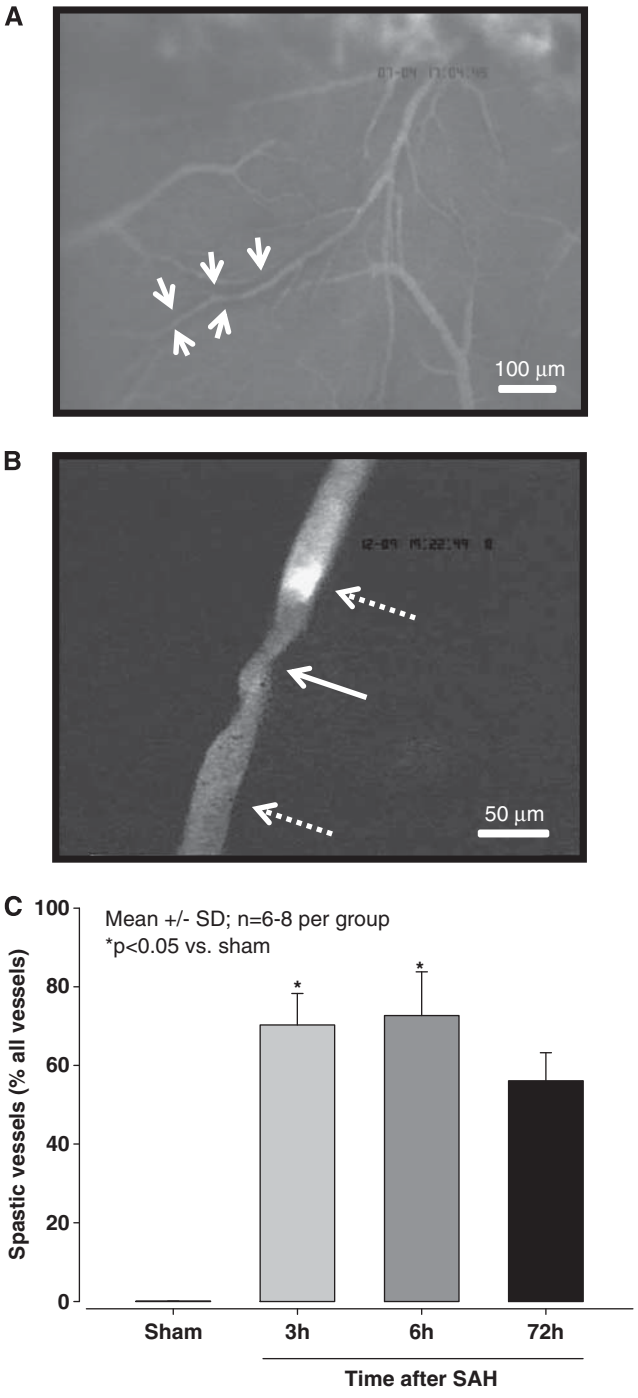

Figure 2 (**A**) Microscopic overview (magnification × 100) of the middle cerebral artery (MCA) territory 3 hours after subarachnoid hemorrhage (SAH). A black halo surrounding some arterioles indicates the presence of subarachnoid blood (white arrows). (**B**) Pearl string-like microarteriolar spasm (solid arrow) in the cerebral microcirculation 3 hours after SAH (magnification × 250). A microthrombus occludes the proximal side of the spasm (upper dotted arrow). (**C**) The proportion of spastic vessels expressed as percent of all vessel segments of the ipsilateral MCA at different time points after SAH ($n = 6$ to 8 per each time point).

did not spread homogenously but accumulated around vessels as identified by a dark margin ensheathing the vessels in the subarachnoid space (Figure 2A, white arrows). About two thirds of all microvessels deriving from the MCA in SAH-induced mice showed this pattern, similar findings were never observed in sham-operated animals (data not shown).

Microvascular Constriction

Three hours after SAH, numerous constricted microvessels were observed. All observed vessels were arterioles; no change of vessel diameter was observed in venules (data not shown). Surprisingly, arteriolar constrictions were not uniform but showed repetitive constrictions approximately every 50 μm along vessels (Figure 2B). This pattern is very similar to the pearl string-like constrictions observed by Uhl *et al* (2003) in SAH patients. No microvascular constrictions were observed in sham-operated mice.

Quantification of these observations revealed that, 3 hours after SAH, 70% of all MCA branches (115 out of 164 investigated vessels) showed one or more constrictions ($P < 0.05$ versus sham). Six hours after SAH, 73% of all vessels deriving from the MCA (99 out of 139 investigated vessels) were constricted ($P < 0.05$ versus sham). Three days after SAH, 91 out of 163 investigated vessels (56%) remained affected by vasoconstriction (Figure 2C). As one vessel branch could display more than one spastic segment, 506 constrictions were found in 305 vessels.

Affected vessel segments constricted by an average of 33 ± 2% 3 hours after SAH ($P < 0.05$ versus sham) and remained constricted for up to 72 hours (Figure 3A). To investigate the distribution of the severity of the observed microvascular constrictions, data were displayed as histograms (Figures 3B and 3C). Three hours after SAH, most vessel segments showed a constriction of 20% to 30%; only around 10% of all vessels showed a very severe (reduction of vessel diameter by −50% to −60%) or very light (reduction of vessel diameter by −10% to −20%) constriction (Figure 3B). This pattern changed over time; 6 hours after SAH, the most severe constrictions occurred less frequently and were not apparent at all at 72 hours, while the number of vessels with a less severe constriction increased by ∼4-fold at 6 and 72 hours after SAH (Figures 3C and 3D).

To investigate which size of arterioles was most affected by vasoconstriction, we analyzed the degree of constriction as a function of vessel diameter. Independent of the investigated time point, small arterioles always demonstrated the most severe constriction (Figures 4A–C), e.g., 3 hours after SAH arterioles with a baseline diameter of 10 to 20 μm constricted by 38.2 ± 2.4% of baseline, while arterioles in the 40 to 80-μm category constricted by only 23.2 ± 1.9%, i.e., almost 40% less ($P < 0.001$; Figure 4A). As already mentioned, arteriolar

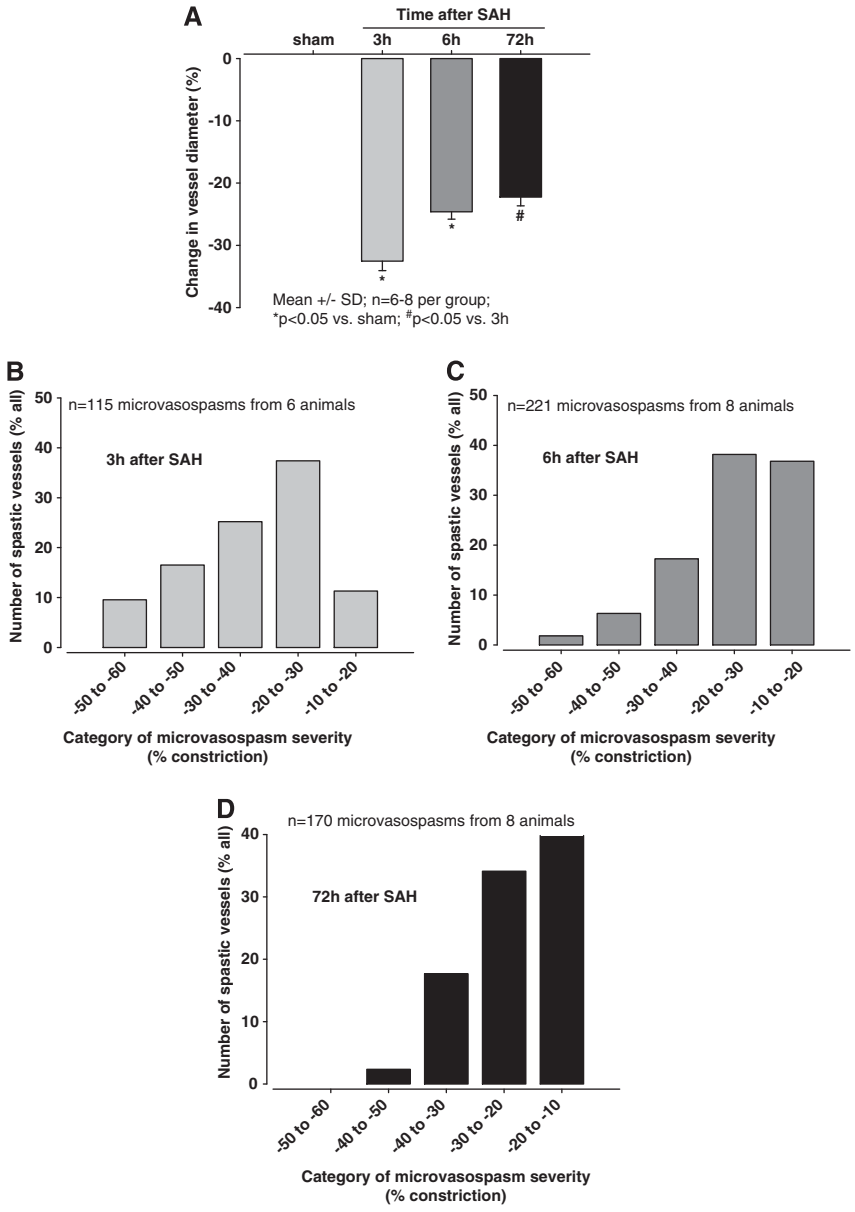

Figure 3 (**A**) Change of vessel diameter in sham-operated animals and at different time points after subarachnoid hemorrhage (SAH) ($n = 6$ to 8 per animal per time point). Histograms showing the distribution of the degree of microvasospasms (**B**) 3 hours, (**C**) 6 hours, and (**D**) 72 hours after SAH.

constriction persisted for at least 3 days after SAH but became somewhat weaker over time. The recovery of arteriolar constriction was, however, not equally distributed over all investigated vessel size categories; recovery was more pronounced in small (10 to 30 μm) as compared with larger vessels (40 to 80 μm) (-20% versus -10%).

Microthrombi

Post hemorrhagic arteriolar constrictions were often associated with severe reductions in microvascular blood flow or even a complete absence of microperfusion. Dynamic imaging of arteriolar constrictions suggests that vessels constrict within seconds thereby causing secondary thrombus formation, i.e., arteriolar constrictions occur first and trigger microthrombosis and not vice versa (Supplementary Video). Complete absence of microvascular flow after SAH was always associated with the formation of thrombi at the proximal end of arteriolar constrictions, as detected by accumulation of FITC-dextran (Figure 5A). Three hours after induction of SAH, 35% of all constricted arterioles carried microthrombi as compared with only $<1\%$ in vessels without spasms ($P<0.001$; Figure 5B). The more pronounced the constriction was, the more microthrombi were

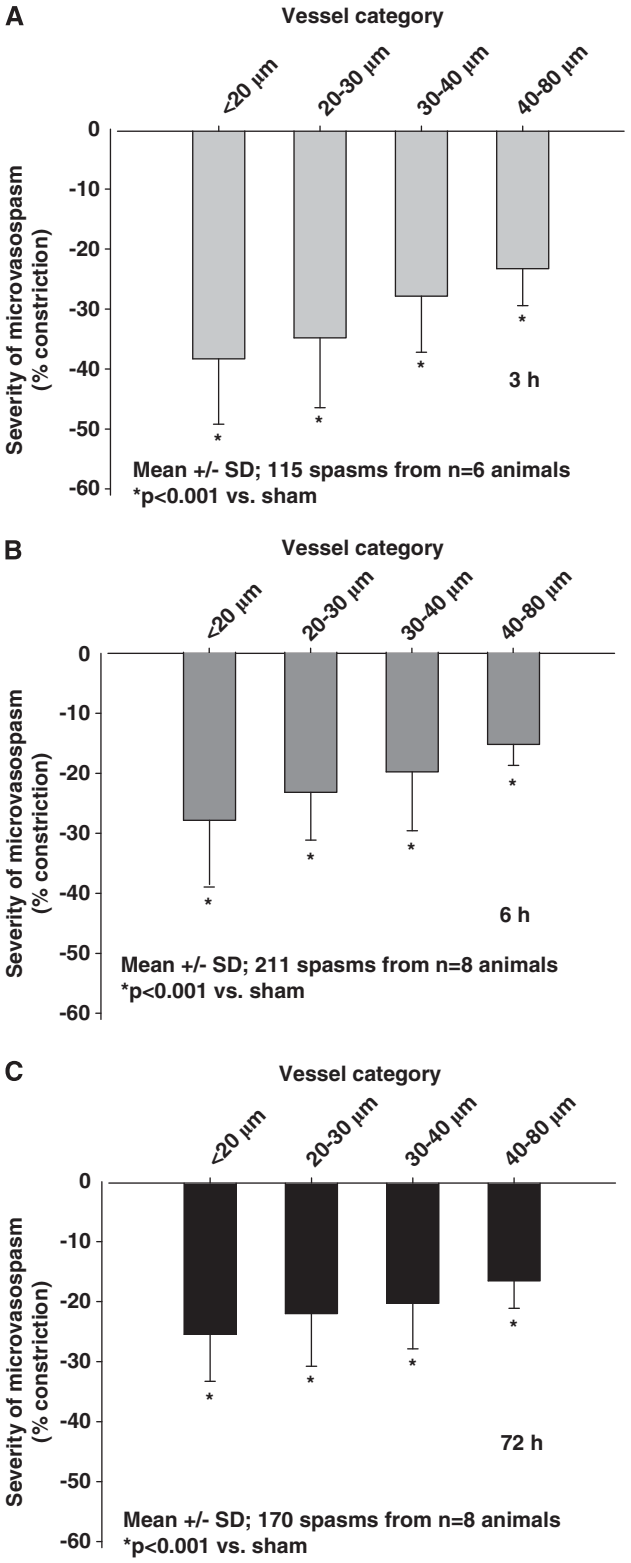

Figure 4 Severity of microarteriolar spasm depending on the baseline diameter of the affected vessels (**A**) 3 hours, (**B**) 6 hours, and (**C**) 72 hours after subarachnoid hemorrhage (SAH). The smallest arterioles are most severely affected by microvasospasm.

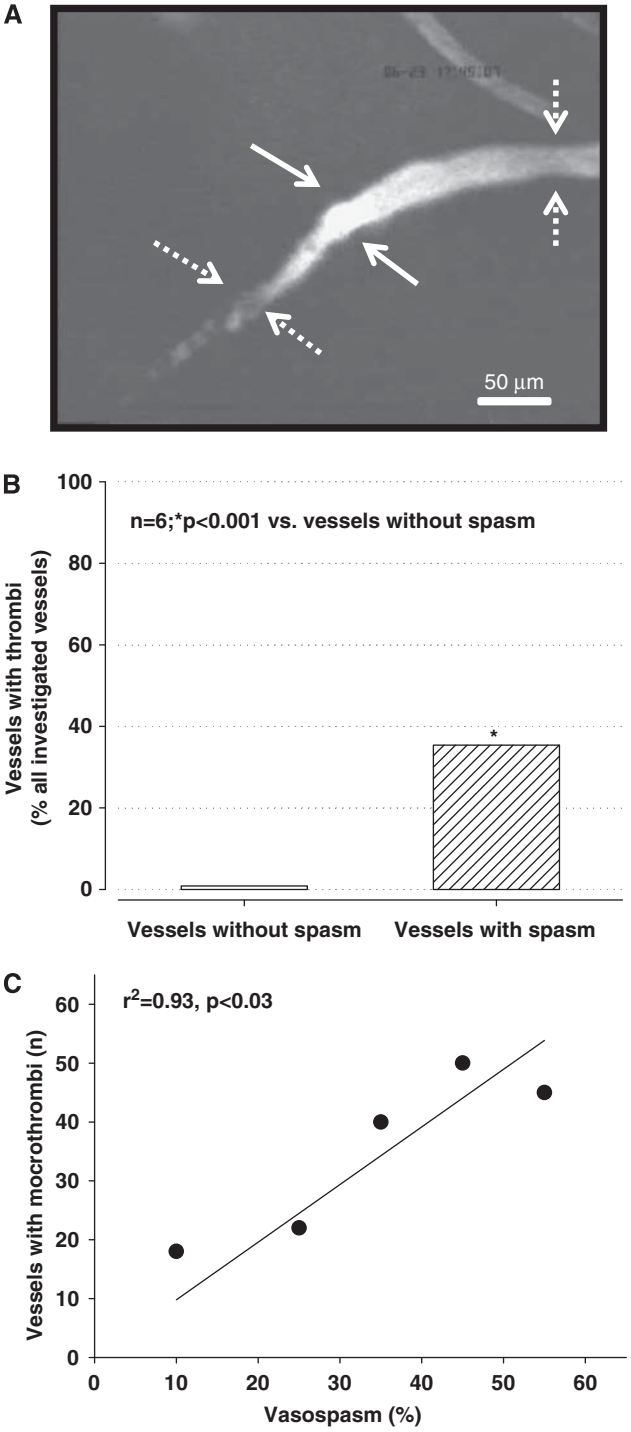

Figure 5 (**A**) Example of a microvessel carrying a large thrombus (solid arrows) between two microvasospasms (dotted arrows). (**B**) Percentage of nonspastic (open bar) and spastic (striped bar) vessels carrying microthrombi 3 hours after subarachnoid hemorrhage (SAH). (**C**) Correlation between the number of microthrombi and microvasospasm severity. The more pronounced microvasospasms were the more microthrombi could be found in the corresponding vessel segments.

present ($r^2 = 0.93$, $P < 0.03$), i.e., only 40 microthrombi were observed in vessels with a constriction of <30%, while 145 microthrombi were found in vessels with a higher degree of constriction (Figure 5C).

Discussion

The aim of the present study was to investigate the long-term spatial and temporal characteristics of acute vasoconstriction after SAH *in vivo*. The main findings of the study are that over 70% of arterioles deriving from the MCA showed pearl string-like constrictions within the first 3 hours after SAH and that these constrictions persisted for at least 3 days after hemorrhage, suggesting that vessels were spastic. Arteriolar diameter was reduced by up to 50% and the more constricted the arterioles were, the more often the vessel lumen was occluded by microthrombosis (30% of all spastic vessels). Since small reductions in arteriolar diameter can significantly reduce blood flow and microthrombosis may stop microperfusion completely, our results may explain the early, CPP-independent severe reduction in cerebral blood flow after SAH in experimental animals and patients (Sehba and Bederson, 2006; Schubert *et al*, 2009).

Subarachnoid hemorrhage patients may already experience cerebral ischemia in the first few days after hemorrhage, when large cerebral vessels do not show any signs of vasospasm (Schubert *et al*, 2009). Since, in most cases, ICP and CPP are in the normal or near normal range in this early post SAH phase, the perfusion deficit has to be attributed to changes at the level of the cerebral microcirculation—as already pointed out by Bederson *et al* (1998), based on experimental findings >10 years ago. This hypothesis was proven experimentally in rats by showing that subarachnoid arterioles indeed constrict by ~40% in the early phase, i.e., 5 minutes to 2 hours after SAH *in vivo* (Sun *et al*, 2009). Vasoconstriction also seems to affect intraparenchymal microvessels as soon as 10 minutes after SAH, as demonstrated by collagen IV and endothelial barrier antigen immunohistochemistry on fixed rat tissue (Sehba *et al*, 2007) and may last up to 7 days as shown using a casting technique in dogs (Ohkuma *et al*, 1997). That the observed changes at the level of the microcirculation are not an experimental artifact, but may indeed contribute to the post hemorrhagic pathophysiology of SAH in humans, were demonstrated by a study performed in our department which visualized the cerebral microcirculation in SAH patients during aneurysm clipping during the first 3 days after the initial bleed, i.e., at time points where macrovasospasm was not present (Uhl *et al*, 2003). Subarachnoid arterioles showed pearl string-like contractions and capillary density was significantly reduced, indicating loss of perfusion at the microcirculatory level after subarachnoid bleeding (Uhl *et al*, 2003). These findings were later confirmed by another group using the same imaging technology (Pennings *et al*, 2004). Based on these experimental and clinical studies, it seems clear that arteriolar constrictions, which remain undetected by routine clinical imaging, may have an important role for the otherwise inexplicable early ischemia occurring after SAH.

Despite this obviously important role of arteriolar constrictions, many questions regarding the pathophysiology of this phenomenon still need to be addressed, e.g., how many vessels are affected, what is the temporal profile of vasoconstriction, which microvessels are mostly affected and is the degree of microvasospasm sufficient to explain ischemic brain damage? The current study helps to answer some of these questions due to technical advantages, which were not previously available. The experiments were performed in an animal model, which resembles clinical SAH as closely as possible, i.e., the endovascular perforation model (Bederson *et al*, 1995; Feiler *et al*, 2010). In analogy to SAH in humans, the endovascular model produces a vascular lesion at the skull base, which results in an immediate increase in ICP, a decrease in CPP and the self-limiting development of a hematoma due to decreasing cerebral blood flow (Bederson *et al*, 1995). Another technical advantage of the current study is that it is one of the few to use intravital videomicroscopy for the direct visualization of the post hemorrhagic cerebral microcirculation *in vivo* (Ishikawa *et al*, 2009; Sun *et al*, 2009). In comparison with previous studies which described post hemorrhagic microvasospasm *ex vivo* by histology on fixed tissue or by casting techniques (Ohkuma *et al*, 1997; Sehba *et al*, 2007), the current study using *in-vivo* microscopy has the intrinsic advantages of studying vessels in the living brain, to be able to study the whole vascular tree of the MCA, to observe dynamic changes, e.g., thrombus formation, and to uncover dynamic interactions, e.g., vasoconstriction and microthrombosis. Finally, the current study was performed in a recently improved mouse SAH model (Feiler *et al*, 2010). Mice have a translucent dura mater and therefore allow the visualization of the subarachnoid/pial microcirculation without durotomy (Kataoka *et al*, 2004; Ishikawa *et al*, 2009; Schwarzmaier *et al*, 2010). This means that the cerebral microcirculation can be visualized without any previous mechanical alterations to the cerebral vasculature and under conditions of physiological cerebrospinal fluid flow. This procedure may explain why this is the first experimental study to observe the pearl string-like pattern of arteriolar constrictions so far only observed in humans (Uhl *et al*, 2003; Pennings *et al*, 2004).

A decrease in microvascular perfusion can be caused by constriction of arterioles or plugging of their lumen by microthrombosis. Our current data demonstrate that both mechanisms are present after SAH *in vivo*, as also suggested by previous studies on

fixed tissue (Ohkuma *et al*, 1997; Sehba *et al*, 2005; Sehba *et al*, 2007). When the cerebral microcirculation is investigated without opening the subarachnoid space, as in the current study and in a previous study using an *ex-vivo* casting technique (Ohkuma *et al*, 1997), post hemorrhagic vasoconstriction seems to occur only in cerebral arterioles, i.e., similar to SAH in patients (Uhl *et al*, 2003; Pennings *et al*, 2004).

Arteriolar constriction occurs in a very high fraction of subarachnoid arterioles (70%) and seems to be severe enough to cause a significant reduction in cerebral blood flow by itself since, according to the Hagen–Poiseuille law, a reduction of vessel diameter by 30% results in a reduction of flow by $\sim$80%, i.e., down to the ischemic threshold. Considering that half of all investigated microvessels have even stronger spastic segments and that small arterioles (which in most cases are end arteries) are the most severely affected by vasoconstriction, the abundance and the degree of arteriolar vasoconstriction alone may be sufficient to explain at least a large part of post hemorrhagic ischemia.

Our results, however, suggest that arteriolar constrictions induce a much more severe microvascular perfusion deficit, namely microcirculatory stasis. As shown by *in-vivo* videomicroscopy, the reduction of arteriolar diameter triggers a most likely secondary, flow reduction-induced formation of apposition thrombi. That low flow, one component of the Virchow trias, is the mechanism of microthrombosis is supported by the fact that the frequency of microthrombus formation correlates very closely with the degree of microarteriolar spasm. If endothelial damage and local adhesion of platelets at the site of the constriction are also involved in this process will need to be addressed in the future. Since these changes occur in subarachnoid/pial arterioles (i.e., at the site of blood deposition) but also in the brain parenchyma (Sehba *et al*, 2005), microvascular constrictions may have a, so far underestimated, role in the pathophysiology of SAH-induced ischemia.

Although we concentrated on the description and quantification of microvascular changes after SAH and did not perform any specific experiments addressing the mechanisms underlying post hemorrhagic microvasospasm, our observations suggest that microvasospasms occur only at sites where the microvasculature comes into direct contact with blood. This may suggest that, among others, hemoglobin, which is known to induce vasoconstriction by scavenging nitric oxide could be involved in this process. Future studies addressing microvascular dysfunction after SAH in detail, e.g., by using nitric oxide donors and other experimental tools, may shed new light on the mechanisms of post hemorrhagic microvasospasm.

Despite the obvious advantages of the experimental approach and the interesting results, the current study also has some limitations that need to be taken into consideration when interpreting the data. Conventional one-photon fluorescence videomicroscopy only allows investigation of superficial structures. Accordingly, the current study provides no information on intraparenchymal vessels and it remains unclear how changes observed in subarachnoid/pial vessels may relate to intraparenchymal alterations. Studies using tissue penetrating two-photon microscopy will be needed to address this issue. Another limitation of the current study is that we focused our interest on the microcirculation and did not investigate large cerebral vessels, which may also show spasm early after hemorrhage in rodents (Bederson *et al*, 1998; Sehba *et al*, 1999). Therefore, we cannot realize if and how acute macrovasospasms and microvasospasms may be linked to each other. Finally, we used an open cranial window preparation for the current experiments, which is equivalent to a decompression craniectomy. Accordingly, we cannot make any statements on the role of intracranial hypertension in the observed microcirculatory changes after SAH. Future experiments using closed cranial window preparations will be needed to address this important issue in detail.

Taken together, the current study shows that *in-vivo* subarachnoid/pial arterioles show the same pearl string-like constrictions that have been previously observed in humans (Uhl *et al*, 2003; Pennings *et al*, 2004), that these constrictions are frequent (70% of all arterioles) and severe enough ($>$30%) to cause ischemia, and that arteriolar constrictions seem to trigger the formation of microthrombosis and microvascular stasis, thereby further aggravating tissue perfusion. Although the detailed molecular mechanisms underlying this phenomenon still need to be investigated, the current results suggest that long-lasting hemodynamic alterations at the microcirculatory level may be an important mechanism for the development of early post hemorrhagic ischemia, which is of utmost im portance for the prognosis of patients experiencing SAH.

Disclosure/conflict of interest

The authors declare no conflicts of interest.

References

Adams Jr HP, Kassell NF, Torner JC, Nibbelink DW, Sahs AL (1981) Early management of aneurysmal subarachnoid hemorrhage. A report of the Cooperative Aneurysm Study. *J Neurosurg* 54:141–5

Bederson JB, Germano IM, Guarino L (1995) Cortical blood flow and cerebral perfusion pressure in a new noncraniotomy model of subarachnoid hemorrhage in the rat. *Stroke* 26:1086–91

Bederson JB, Levy AL, Ding WH, Kahn R, DiPerna CA, Jenkins III AL, Vallabhajosyula P (1998) Acute vasoconstriction after subarachnoid hemorrhage. *Neurosurgery* 42:352–60

Cahill J, Zhang JH (2009) Subarachnoid hemorrhage: is it time for a new direction? *Stroke* 40:S86–7

Feiler S, Friedrich B, Schöller K, Thal SC, Plesnila N (2010) Standardized induction of subarachnoid hemorrhage in mice by intracranial pressure monitoring. *J Neurosci Methods* 190:164–70

Harrod CG, Bendok BR, Batjer HH (2005) Prediction of cerebral vasospasm in patients presenting with aneurysmal subarachnoid hemorrhage: a review. *Neurosurgery* 56:633–54

Herz DA, Baez S, Shulman K (1975) Pial microcirculation in subarachnoid hemorrhage. *Stroke* 6:417–24

Ishikawa M, Kusaka G, Yamaguchi N, Sekizuka E, Nakadate H, Minamitani H, Shinoda S, Watanabe E (2009) Platelet and leukocyte adhesion in the microvasculature at the cerebral surface immediately after subarachnoid hemorrhage. *Neurosurgery* 64:546–53

Kataoka H, Kim SW, Plesnila N (2004) Leukocyte-endothelium interactions during permanent focal cerebral ischemia in mice. *J Cereb Blood Flow Metab* 24:668–76

Ohkuma H, Itoh K, Shibata S, Suzuki S (1997) Morphological changes of intraparenchymal arterioles after experimental subarachnoid hemorrhage in dogs. *Neurosurgery* 41:230–5

Pennings FA, Bouma GJ, Ince C (2004) Direct observation of the human cerebral microcirculation during aneurysm surgery reveals increased arteriolar contractility. *Stroke* 35:1284–8

Pluta RM, Hansen-Schwartz J, Dreier J, Vajkoczy P, Macdonald RL, Nishizawa S, Kasuya H, Wellman G, Keller E, Zauner A, Dorsch N, Clark J, Ono S, Kiris T, Leroux P, Zhang JH (2009) Cerebral vasospasm following subarachnoid hemorrhage: time for a new world of thought. *Neurol Res* 31:151–8

Pobereskin LH (2001) Incidence and outcome of subarachnoid haemorrhage: a retrospective population based study. *J Neurol Neurosurg Psychiatry* 70:340–3

Schöller K, Feiler S, Anetsberger S, Kim S-W, Plesnila N (2011) Contribution of bradykinin receptors to the development of secondary brain damage after experimental subarachnoid hemorrhage. *Neurosurgery* 68:1118–23

Schubert GA, Seiz M, Hegewald AA, Manville J, Thome C (2009) Acute hypoperfusion immediately after subarachnoid hemorrhage: a xenon contrast-enhanced CT study. *J Neurotrauma* 26:2225–31

Schwarzmaier SM, Kim SW, Trabold R, Plesnila N (2010) Temporal profile of thrombogenesis in the cerebral microcirculation after traumatic brain injury in mice. *J Neurotrauma* 27:121–30

Sehba FA, Bederson JB (2006) Mechanisms of acute brain injury after subarachnoid hemorrhage. *Neurol Res* 28:381–98

Sehba FA, Ding WH, Chereshnev I, Bederson JB (1999) Effects of S-nitrosoglutathione on acute vasoconstriction and glutamate release after subarachnoid hemorrhage. *Stroke* 30:1955–61

Sehba FA, Friedrich Jr V, Makonnen G, Bederson JB (2007) Acute cerebral vascular injury after subarachnoid hemorrhage and its prevention by administration of a nitric oxide donor. *J Neurosurg* 106:321–9

Sehba FA, Mostafa G, Friedrich Jr V, Bederson JB (2005) Acute microvascular platelet aggregation after subarachnoid hemorrhage. *J Neurosurg* 102: 1094–100

Strahler AN (1944) Geomorphic significance of valleys and parks of the Kaibab and Coconino plateaus, Arizona. *Science* 100:219–20

Sun BL, Zheng CB, Yang MF, Yuan H, Zhang SM, Wang LX (2009) Dynamic alterations of cerebral pial microcirculation during experimental subarachnoid hemorrhage. *Cell Mol Neurobiol* 29:235–41

Thal SC, Plesnila N (2007) Non-invasive intraoperative monitoring of blood pressure and arterial pCO2 during surgical anesthesia in mice. *J Neurosci Methods* 159:261–7

Uhl E, Lehmberg J, Steiger HJ, Messmer K (2003) Intraoperative detection of early microvasospasm in patients with subarachnoid hemorrhage by using orthogonal polarization spectral imaging. *Neurosurgery* 52:1307–15

Weir B, Grace M, Hansen J, Rothberg C (1978) Time course of vasospasm in man. *J Neurosurg* 48:173–8

Supplementary Information accompanies the paper on the Journal of Cerebral Blood Flow & Metabolism website (http://www.nature.com/jcbfm)